Design and realization of a wireless self-resonant power transmission device based on a differentiator circuit to command the power switches of a primary series resonant circuit

Fekou Kuekem Narcisse, Ndjiya Ngasop, and Alexis Kuitche

Abstract-- The work carried out consists to design and realize a wireless and self-resonant energy transmission device. To design our device, we make used of Pspice 9.2 simulation software. The realization is done on a printed circuit board. Voltages is been visualize through a 200MHz analog oscilloscope. The approach used to implement our auto-resonant device is based on the differentiation of the output voltage in view of command. To this end a literature review is done in other to know the previous work in the domain. From this literature review, we notice that most of the previous device use lock phase loops but none of them address the self-resonant principle. Nevertheless we face an important difficulty, namely the bandwidth of our operational amplificatory that was lower than the MHz, this then reduces the frequency of our device to a maximum of 50MHz.

Keys words-- Coupling, Current source, Differentiator, Inverter, Power switches, Resonance, Zero current control.

1 INTRODUCTION

IN 2007, using an inductive resonant coupling, wireless power transmission systems were revolutionize by the team of witricity [1], [2]. This coupling is based on the principle of flux transfer from an emitting coil (primary), to a receiving coil (secondary). Both are connected each one to a capacitor, enabling a resonant functioning (see figure 1).

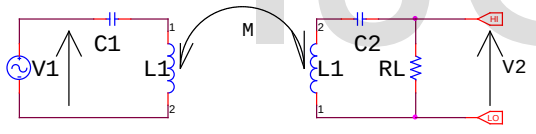

Fig. 1. Schematic diagram of a resonant coupling, [1], [2], [6].

In order to obtain a good efficiency, it is necessary that: the source V1, the primary resonant circuit (C1, L1), and the secondary resonant circuit (C2, L2), are fully in frequencies tuning [3], [7].

Furthermore, to reach important powers and lower losses, the input voltage V1 has to be a square or a rectangular voltage, giving by an inverter [4]. To realize that inverter, the "push pull" assembly is been mostly used. Its structure is represented as follow [4]:

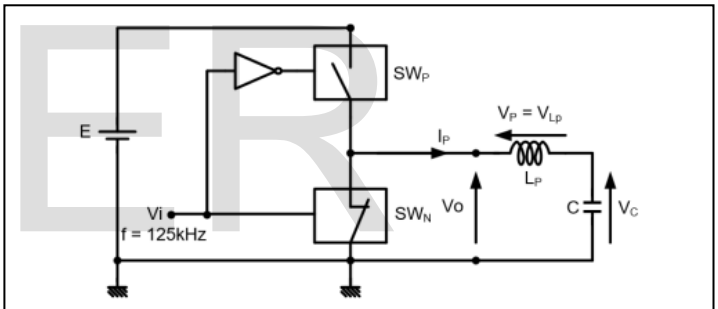

Fig. 2. Schematic diagram of a push-pull inverter series resonant circuit [4].

While neglecting losses by joule effect, theoretical study shows an increase of 2E each period.

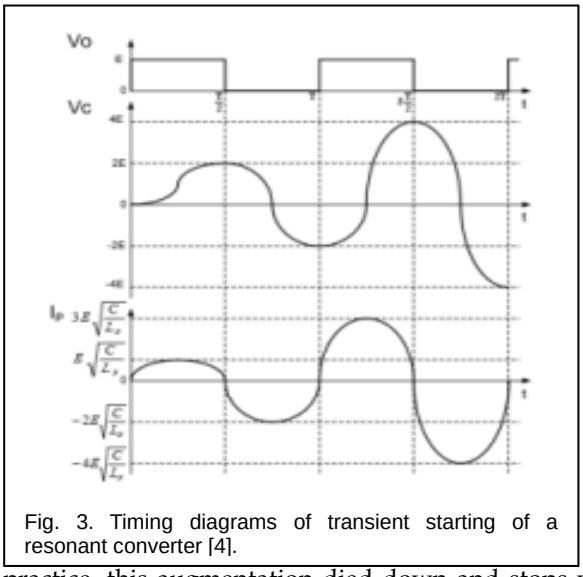

Fig. 3. Timing diagrams of transient starting of a resonant converter [4].

In practice, this augmentation died down and stops when

- *Fekou Kuekem Narcisse, Department of Electrical Engineering, Energy and Automation, National School of Agro-Industrial Sciences (ENSAI), University of Ngaoundere, Cameroon, PH-00237699564181. E-mail: fekou2002@yahoo.fr*
- *Ndjiya Ngasop, Department of Electrical Engineering, Energy and Automation, National School of Agro-Industrial Sciences (ENSAI), University of Ngaoundere, Cameroon, PH-00237677391749. E-mail: ndjiyangasop@yahoo.fr*
- *Kuitche Alexis, Department of Electrical Engineering, Energy and Automation, National School of Agro-Industrial Sciences (ENSAI), University of Ngaoundere, Cameroon. E-mail: kuitche_a@yahoo.fr*

the energy accumulated through a period is equal to the energy loss through that same period.

Aiming to reduce conduction losses, the power switches of the inverter should be command when the current is null. For this reason, almost all the authors propose:

1. Either the adjustment of the frequency of the input signal to the inherent frequency of the resonant circuit, which is very approximate and tedious [5], [8], [10], [11], [12];
2. Or the lock phases system which is very effective but of a complex realization [4], [9].

In this article, we propose a simple method of command based on the differentiation of the output voltage. From the timing diagrams of figure 3, we see as a matter of fact that the current being a function of the derivative of the voltage across the capacitor, follows the same profile as the control voltage.

2 MATERIAL

In this article, we have used **Pspice 9.2** as simulations software. The practical curves have been visualized through an analog oscilloscope of 20MHz.

3 METHODS

3.1 Principle

The global principle of our study respects the block diagram represented below:

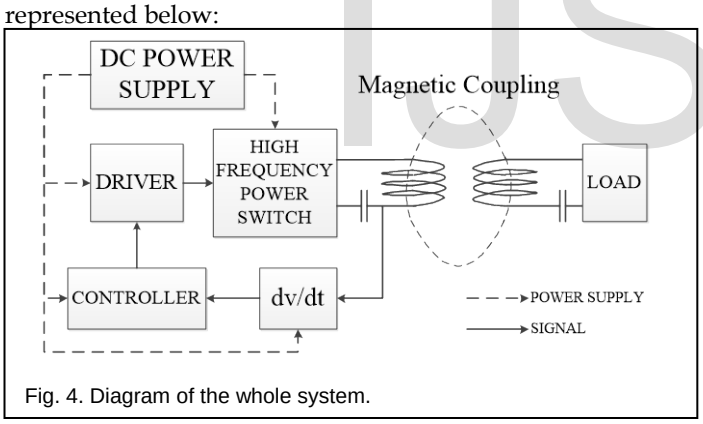

Fig. 4. Diagram of the whole system.

The functioning of our system is described as follow:

At the beginning, the power system sends a positive voltage to the primary resonant circuit. This resonant circuit therefore starts oscillating, from there, a sinusoidal voltage is generated. That voltage is derived (in order to obtain a quantity proportional to the current), then shaped by the controller before being pre-amplify by the driver in order to command high frequency power switches when current is null in the primary resonant circuit. This principle enabled the system to function no matter the resonance frequency. However we choose a frequency of 16 KHz for the tests, from this block diagram, we obtained the following global diagram.

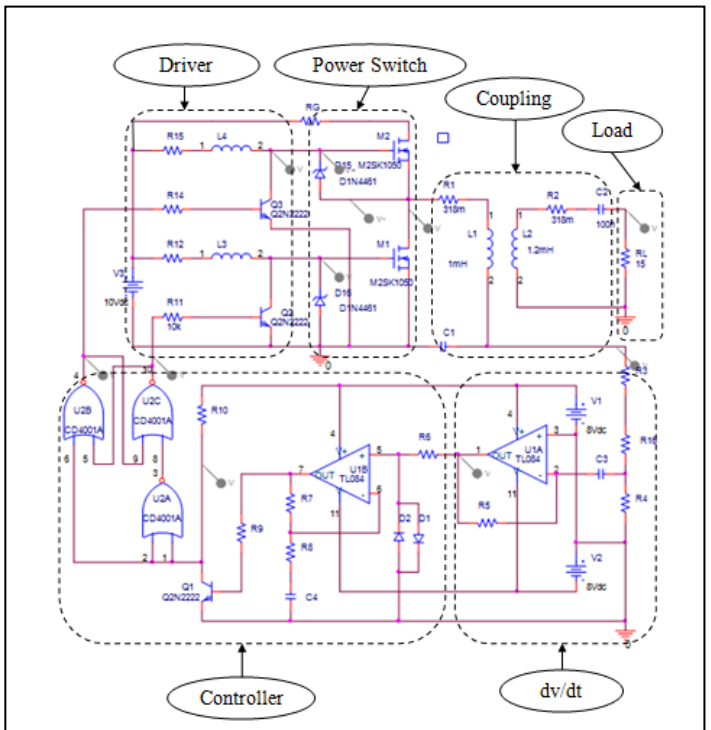

Fig. 5. Global diagram of the system.

Let us introduce now the different blocks of our system

3.2 Current To Voltage converter $I_C = C\,(dV_C)/(dt)$

Our study is based on the principle which says that the current across a series resonant LC circuit is null when the voltage is maximal. In fact, in such circuit, current and voltage are in quadrature of phases. We develop this approach since it is very complex to measure the current in such a circuit. Because adding a series resistance [6], across which tapping voltage proportional to the current will considerably reduce the efficiency.

Nevertheless, it is possible to find out this current simply by deriving the voltage either across the inductor or across the capacitor terminals. This can be done through a simple reverser differentiator with an operational amplifier.

The output voltage of this differential inverter is expressed by $V_s = -RC(dV_e)/(dt)$, this relation remains true while the operational amplifier function in linear regime. That is, for $|V_S| < |V_{CC}|$ which implies $RC\omega\hat{V}_e < V_{CC}$. Figure 6 gives the timing diagrams of input voltages (Vi) and output voltages (Vd) of the differentiator.

3.3 The controller or shaping circuit

The controller is use to shape the signal from the differentiator, in order to obtain two square and two-phased signals necessary for the command of high frequency power switches. The square signal Va of figure 6 obtained by the very high amplification of the voltage gain, while the two-phased signals (Vb1, Vb2) are obtained from an RS bi-stable flip-flop.

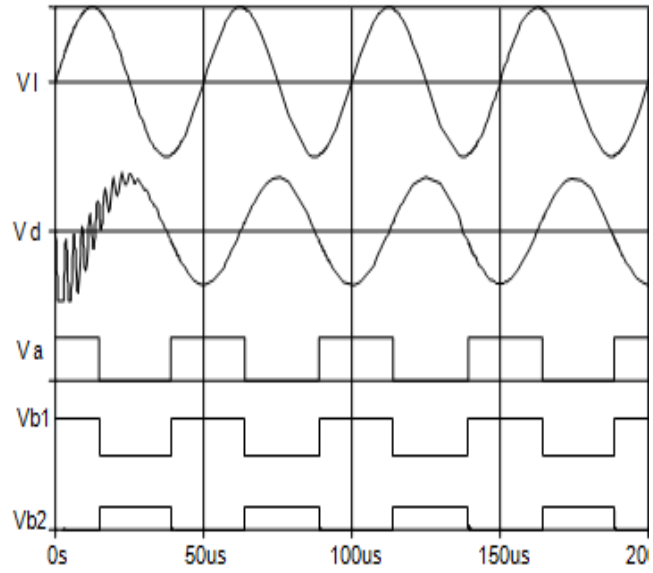

Fig. 6. Timing diagrams of voltage Vi (input signal of the differentiator), Vd (derived voltage), Va (amplified voltage), Vb1 and Vb2 (bi-phased voltage one and two).

3.4 Drivers of Power switches

To realize those drivers, we used current sources due to the simplicity to realize them and the possibility they offers to produce overvoltage enabling the quasi-simultaneous control of floating grills. These current sources have been realized with the self of great inductance so that current variations will be negligible. The grill-source junction being assimilable to a capacitor, its charge equation with constant current is similar to a straight line (figure 7: VGSM1 and VGSM2). In fact:

$$v_{GS} = \int_0^t \frac{I_0}{C_{GS}} dt = \frac{I_0}{C_{GS}} t + V_{GS_0} = \frac{I_0}{C_{GS}} t \qquad (1)$$

With:

T: time

V_{GS}: grill source voltage;

$V_{GS0} = 0$: grill source voltage at the beginning of each load;

C_{GS}: capacity of the grill source junction;

I_0: constant current produced by each of the inductors.

In order to reduce losses due to commutation, the duration of commutation should be minimized. This bring to reduce the time necessary for the voltage VGS to leave from 0V to $v_{GS\,on} = 5V$. Lets suppose that this time $t = T_{on} = 1\mu s$, the current I_0 of the current source necessary to obtain this time will be:

$$I_{0min} = \frac{v_{GS\,on} * C_{GS}}{T_{on}} = \frac{5 * 1.5 * 10^{-9}}{10^{-6}} = 7.5mA \qquad (2)$$

A ZENER diode mounted in parallel with the grill source junction of power MOSFET, does not only permit to protect this junction but also limit energy losses of the current source.

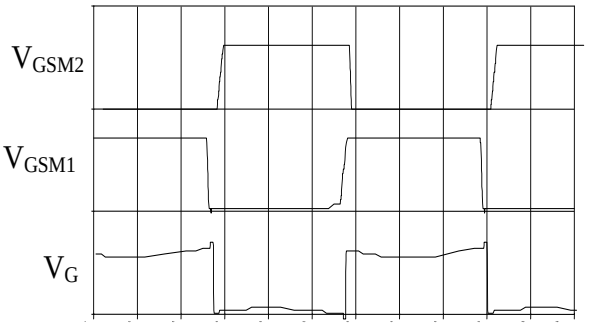

Fig. 7. Voltage Timing diagrams of grill-source junctions of the two powers MOSFET (V_{GSM1}, V_{GSM2}) and that of the voltage including ripple.

3.5 Inductive coupling

It is made up on one side of a real coil (L1, R1) and of a capacitor of frequency tuning (C1) at the primary and on the other side of a real coil (L2, R2) and of a capacitor of frequency tuning (C2) at the secondary as seen on figure 8.

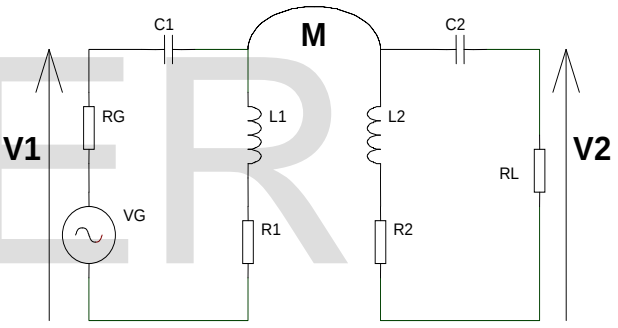

$C_1 = C_2 = C = 100\ nF;\ L_1 = L_2 = L = 1\ mH;$

$\omega_0 = \frac{1}{\sqrt{LC}} = 100\,000\ rad/s\ ;$

$R_1 = R_2 = R = 300\ m\Omega;\quad R_L = 14\Omega;$

$R_G = 320\ m\Omega;\quad R_L = 14\Omega$

Fig. 8. Resonant inductive bondage.

The primary and the secondary should have the same frequency of resonance, thus:

$$\omega = \frac{1}{\sqrt{L_1 C_1}} = \frac{1}{\sqrt{L_2 C_2}} = \frac{1}{\sqrt{LC}}. \qquad (3)$$

In order to command the power MOSFETs at the moment when the current in the primary resonator is null, the voltage VG coming from the inverter (also called power switches) has thus to be, not only in perfect agreement with the resonance frequency, but also in quadrature-phase with the voltage across the capacitor, as seen on the chronogram of simulation on figure 9.

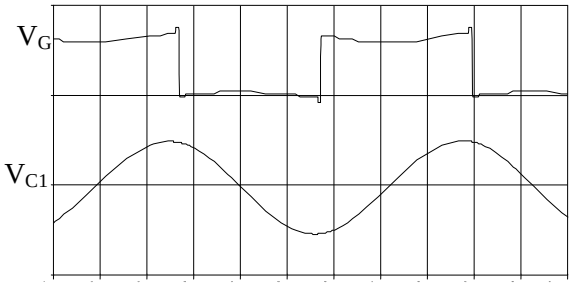

Fig. 9. Digital timing diagram at the inverter output (VG) and the primary voltage (V_{c1}).

4 RESULTS

4.1 Picture of the device

The mounting was realized on a printed circuit board (figure 10), while the coupling components were placed on a guiding device in translation (graduated in centimeters) so as to have a null misalignment (figure 11).

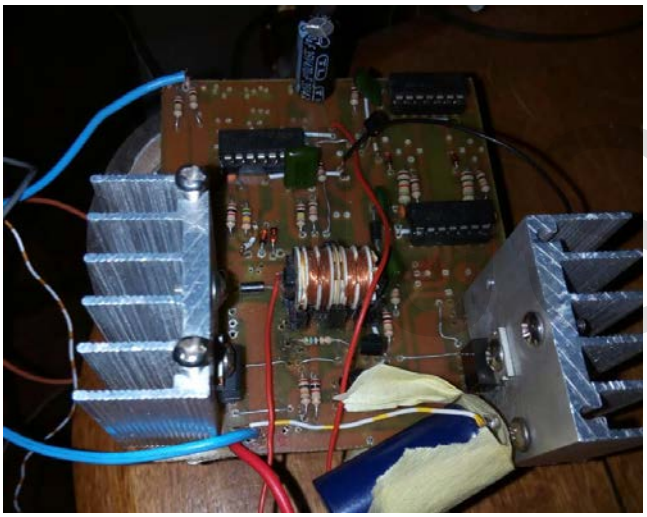

Fig. 10. Electronic card of the system.

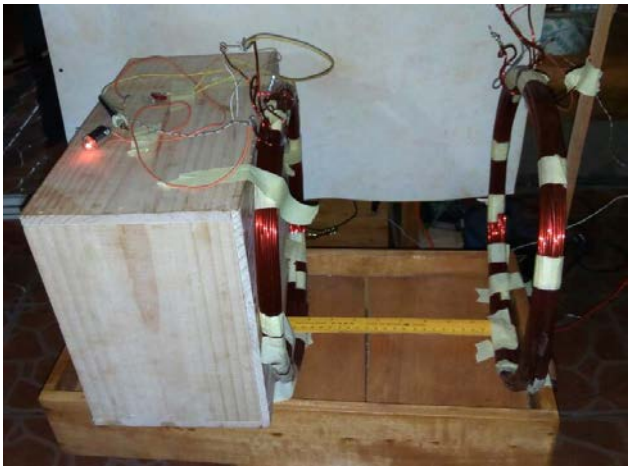

Fig. 11. Coupling placed on a on a guiding device (graduated in centimeters).

4.2 Output signal

The tests that were carried out shows clearly that the voltage including ripple VG is in quadrature of phase with the voltage VC1 (figure 12). For a distance of 17cm, we obtained an output voltage of 3V (figure13). In addition, those two voltages are in phase, which shows that the primary and the secondary circuits resonate at the same frequency.

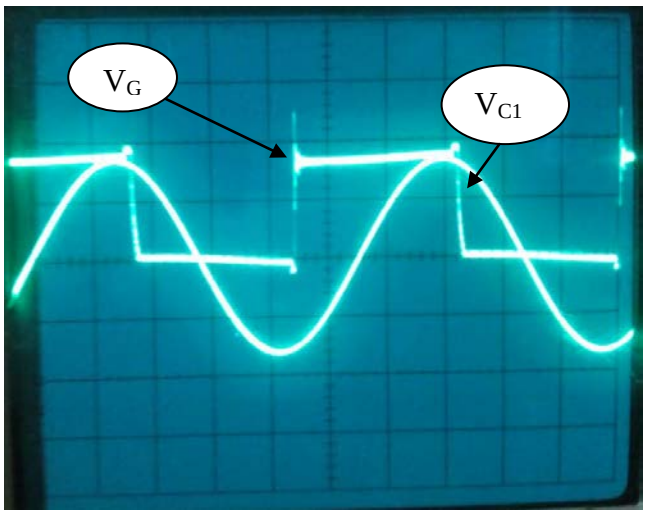

Fig. 12. Chronogram of the inverter output voltage VG and across the primary capacitor VC1. Where V_G: Calibrated at 5V/div in the y axis and 10µs/div in the X axis; and V_{C1}: Calibrated at 50V/div in the y axis and 10µs/div the X axis

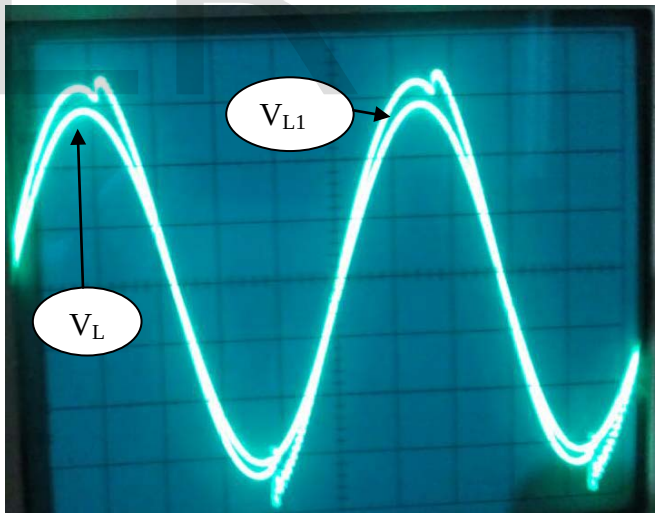

Fig. 13. Chronogram of primary coil voltage VL1 and of the load VL. Where V_{L1}: Calibrated at 50V/div in the y axis and 10µs/div in the X axis; and V_L: Calibrated at 1V/div in the y axis and 10µs/div in the X axis.

4.3 Efficiency

To evaluate the performances of the device, a series of measurements were made by varying the distance between the coils, from 3 to 44cm in steps of 1cm. From these measures, the following graphs were drawn with respect to that distance (D), where K is the coupling coefficient graduated on the y axis to the right of each curves.

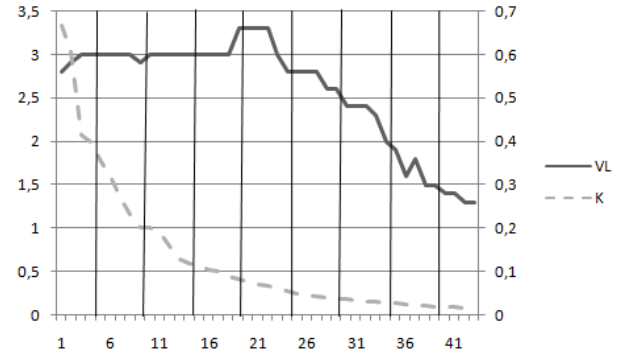

Fig. 14.: Evolution of the load voltage VL with respect to distance D.

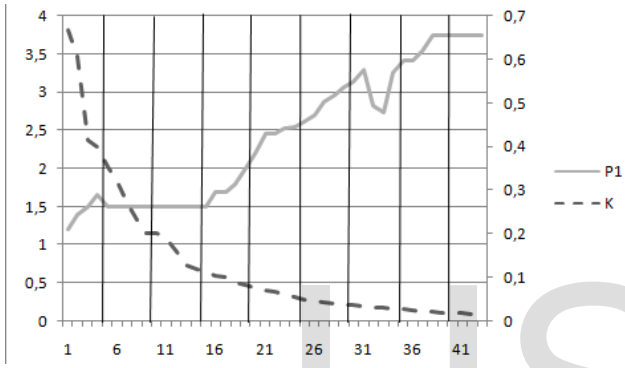

Fig.15. Evolution of absorbed power P1 with respect to distance D

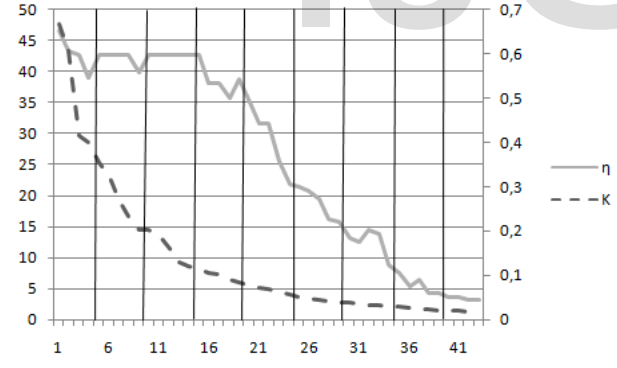

Fig. 16. Evolution of the efficiency η with respect to distance D

5 Discussions

From these curves, three observations were made:

1. Output voltages keeps a considerable value up to about 30cm corresponding to the diameter of each coil, with a maximum between 20 and 23cm;
2. The power absorbed by the device is greater at no load than with load;
3. Contrary to voltage, the efficiency reduces considerably as from 17cm.

To minimize losses in such a system, it is therefore necessary to always make it to function in charge because at no load, the losses are maximal.

6 Conclusion

In a nutshell, we were to design and realize a device of wireless power transmission through self-resonance. We can say that the aim of this study is fulfill. In addition, since this principle does not use the input signal, it is reliable and can function for all the frequency of operational amplifier bandwidth though this bandwidth is reduced. It will be of a great interest in the future to see how to increase that bandwidth.

References

[1] A. Karalis, J. D. Joannopoulos, and M. Soljacic, "Efficient wireless non-radiative mid-range energy transfer," Ann. Phys., vol. 323, pp. 34–48, Avril 2007

[2] Kurs A, Karalis A, Moffatt R, Joannopoulos JD, Fisher P and Soljacic M, Wireless power transfer via strongly coupled magnetic resonances, Jul 6;317(5834):83-6. Epub 2007 Jun 7.

[3] S. L. Ho, Junhua Wang, W. N. Fu , and Mingui Sun , A Comparative Study Between Novel Witricity and Traditional Inductive Magnetic Coupling in Wireless Charging, IEEE 5, MAY 2011

[4] [Megd_2011] Megdouda MANSEUR, Contribution A L'étude D'un Système De Biotélémesure Intracorporelle Par Gélule Ingérable, L'université Bordeaux 1, Ecole Doctorale Des Sciences Pour L'Ingénieur, Décembre 2011

[5] Wei Ting Chen, Raoul A. Chinga, Shuhei Yoshida, Jenshan Lin, and Chao-Kai hsu ; A 36 W Wereless Power Transfer System with 82% Efficiency for led Lighting Applications. 25 Octobre 2013

[6] Morris Kesler, Highly Resonant Wireless Power Transfer : Safe, Efficient, and over distance, witricity cooportion 2013

[7] Heinz Zenkner, Werachet Khan-Ngern, Energy Transfer by Resonance Coupling (IJECE) Vol. 3, No. 5, October 2013, pp.

[8] Ping-an Tan, Haibing He, and Xieping Gao, A Frequency-Tracking Method Based on SOGI-PLL for Wireless Power Transfer System to Assure Operation in Resonant State, Xiangtan University, Xiangtan, China, 2014

[9] Aref TERGUI. asservissement de l'énergie inductive transmise aux implants électroniques. Département de génie électrique école polytechnique de Montréal, Janvier 2014.

[10] Prashana, Aditya Duggal, Manish Kumar Srivastava. An Innovative Disign of Wireless Power Transfer by High Frequency Resonant Coupling, International Journal of Innovative Research in Science, Engineering and Technology. Vol. 4 Issue 7, july 2015

[11] [Mehd_2015] Mehdi Niroomand, Mahbubeh Lotfian. A wireless based power transmission to supply deep brain stimulators. Department of Electrical Engineering, University of Isfahan (UI), Isfahan, Iran. 24 April 2015.

[12] Richard N. Anthony, Seema P. Navghare Student M.E. (Electrical Power System), Introduction To Wireless Power Transfer, International Journal of Scientific Engineering and Applied Science (IJSEAS) – Volume-2, Issue-1, January 2016.